

# Cordycepin ameliorates brown adipose tissue whitening induced by long-term continuous light exposure *via* the AMPK/PGC-1 $\alpha$ /UCP1 signaling pathway

Ruonan Zhang<sup>1,2#</sup>, Li Zhang<sup>2#</sup>, Yuqing Jiang<sup>1,2</sup>, Zhiwei Zhao<sup>1,2</sup>, Guanyu Zhang<sup>2</sup>, Yongqiang Zhang<sup>2</sup>, Shuai Wu<sup>2</sup>, Xi Li<sup>2\*</sup>, Danfeng Yang<sup>2\*</sup>

## Abstract

**Background:** Long-term exposure to light has emerged as a novel risk factor for metabolic diseases. The whitening of brown adipose tissue (BAT) may play an important role in metabolic disorders caused by long-term continuous light exposure. This study aimed to investigate the morphological and functional alterations in BAT under continuous light conditions and to identify traditional Chinese medicine compounds capable of reversing these changes. **Methods:** A metabolic disorder model was established by subjecting mice to continuous light exposure for 5 weeks. During this period, body weight, food intake, and body fat percentage were monitored. Serum levels of triglyceride (TG), total cholesterol (TC), high density lipoprotein cholesterol (HDL-C), and low density lipoprotein cholesterol (LDL-C) were measured to assess lipid metabolism. Histological changes in BAT were examined using H&E staining. The expression of the thermogenic marker uncoupling protein 1 (UCP1) in BAT was determined by RT-qPCR and Western blot to evaluate thermogenic function. RNA sequencing (RNA-seq) was employed to identify differentially expressed genes (DEGs) involved in BAT whitening induced by prolonged continuous light exposure. DEGs were analyzed using the connectivity map (CMap) database to identify potential preventive and therapeutic compounds. The therapeutic efficacy of the selected compounds was subsequently evaluated using the above indicators, and key pathways were validated through western blot analysis. **Results:** After 5 weeks of continuous light exposure, mice exhibited increased body fat percentage and serum levels of TG, impaired mitochondrial function, reduced thermogenic capacity, and whitening of BAT. Gene ontology (GO) and Kyoto encyclopedia of genes and genomes (KEGG) enrichment analyses indicated that BAT whitening was primarily associated with the adenosine 5'-monophosphate-activated protein kinase (AMPK) signaling pathway, fatty acid metabolism, and circadian rhythm. Ten hub genes identified using Cytoscape were mainly related to AMPK signaling and heat shock proteins. *In vivo* experiments showed that cordycepin significantly attenuated the increase in body fat percentage caused by prolonged light exposure. This effect was mediated by activation of the AMPK/PGC-1 $\alpha$ /UCP1 signaling pathway, which restored the multilocular morphology and thermogenic function of BAT. **Conclusion:** Cordycepin mitigates continuous light-induced BAT whitening and metabolic disturbances by activating the AMPK signaling pathway.

## Keywords

long-term continuous light; brown adipose tissue; whitening; cordycepin; AMPK

Received 21 Feb 2025, accepted 09 May 2025

<sup>1</sup>School of Graduate Studies, Tianjin University of Traditional Chinese Medicine, Tianjin 301617, China

<sup>2</sup>Academy of Military Medical Sciences, Academy of Military Sciences, Tianjin 300050, China

\*Corresponding authors Danfeng Yang, E-mail: fengdyd@126.com; Xi Li, E-mail: woshiliulangdeyu@163.com

#These authors contributed equally to this work

Open Access. © 2025 The author (s), published by De Gruyter on behalf of Heilongjiang Health Development [CC BY] Research Center. This work is licensed under the Creative Commons Attribution 4.0 International License.

## 1 Introduction

The polar regions, comprising the Arctic and Antarctic, are critical

components of the Earth's ecosystem. They play a vital role in global climate regulation, biodiversity conservation, natural resource management, and scientific exploration. However,

these regions are marked by extreme environmental conditions, including intense cold, strong winds, high ultraviolet radiation, and unique photoperiodic phenomena such as polar day and polar night. These abnormal light-dark cycles, in particular, have been shown to induce sleep disturbances, cognitive impairment, and mood disorders among personnel stationed in these areas, significantly compromising their operational efficiency and well-being<sup>[1-3]</sup>. Moreover, epidemiological studies have identified a positive correlation between prolonged light exposure and elevated body mass index (BMI), with longer durations of light exposure being associated with increased risks of obesity, diabetes, and other metabolic disorders<sup>[4]</sup>. These findings underscore the importance of elucidating the mechanisms underlying metabolic imbalances caused by continuous light exposure and identifying safe and effective preventive and therapeutic strategies.

Brown adipose tissue (BAT) plays a crucial role in maintaining metabolic homeostasis in humans<sup>[5]</sup>. Unlike white adipose tissue (WAT), which primarily stores energy, BAT specializes in energy expenditure and thermogenesis. It is mainly located in the interscapular region and is characterized by multilocular lipid droplets and a high density of mitochondria<sup>[6]</sup>. These mitochondria contain uncoupling protein 1 (UCP1), a distinctive protein that uncouples oxidative phosphorylation from adenosine triphosphate (ATP) synthesis, dissipating the proton gradient as heat. This non-shivering thermogenesis contributes significantly to the maintenance of energy balance and body temperature<sup>[7]</sup>.

BAT can undergo a phenotypic transformation known as "whitening" under specific pathological or environmental conditions, including high-fat diets, aging, thermoneutral ambient temperatures, and exposure to certain pharmacological agents such as glucocorticoids<sup>[8-11]</sup>. Whitening is marked by the accumulation of large unilocular lipid droplets, hypertrophy of adipocytes, mitochondrial dysfunction, and downregulation of UCP1 expression. These alterations reduce the thermogenic capacity of BAT, lower overall energy expenditure, and contribute to a positive energy balance, thereby increasing susceptibility to obesity, diabetes, and related metabolic disorders. Notably, prolonged light exposure has also been reported to suppress BAT thermogenesis and induce whitening<sup>[12]</sup>. However, the molecular mechanisms underlying BAT whitening caused by continuous light exposure remain largely unclear.

RNA sequencing (RNA-seq) has emerged as a powerful tool for comprehensive transcriptomic analysis, offering deep insights into gene expression changes associated with disease states and therapeutic interventions<sup>[13-15]</sup>. In parallel, the connectivity map (CMap) database enables the identification of bioactive compounds and therapeutic candidates based on gene expression signatures. This resource facilitates the discovery of

potential pharmacological interventions by mapping relationships among genes, diseases, and drugs<sup>[16]</sup>.

In this context, the present study aims to investigate the molecular mechanisms underlying BAT whitening induced by prolonged continuous light exposure using RNA-seq. We further leverage the CMap database to screen for potential therapeutic agents, with a particular focus on traditional Chinese medicine (TCM) monomer compounds. Finally, we validate the effects of the selected compound *in vivo* to assess its therapeutic potential in preventing or reversing BAT whitening.

## 2 Materials and methods

### 2.1 Establishment of animal models

Male C57BL/6J mice (Beijing Vital River Laboratory Animal Technology Co., Ltd., Beijing, China) were housed under standard laboratory conditions with free access to food and water. Mice were randomly divided into two groups ( $N = 10$  per group). The control group (LD) was maintained under a 12 h:12 h light-dark cycle, while the experimental group (LL) was exposed to continuous light (24 h: 0 h light-dark cycle) for five weeks. During this period, body weight and food intake were recorded weekly. At the end of the exposure period, mice were sacrificed, and blood and interscapular BAT were collected for further analysis. All procedures involving animals were conducted in accordance with the regulations of the Institute of Military Medical Sciences Academy and were approved by the Experimental Animal Ethics Committee (IACUC of AMMS-04-2023-034).

### 2.2 Body composition analysis

Following the modeling period, mice were anesthetized with isoflurane and placed on the scanning platform. Whole-body fat percentage was assessed using the InAlyzer body composition analyzer (Osteosys, Korea).

### 2.3 Blood biochemistry analysis

Fresh blood samples were collected and centrifuged at 3500 rpm for 15 min. Serum was carefully isolated and analyzed using an automatic biochemical analyzer (Rayto Life and Analytical Sciences Co., Ltd. Shenzhen, China). The serum levels of triglyceride (TG), total cholesterol (TC), high density lipoprotein cholesterol (HDL-C), and low density lipoprotein cholesterol (LDL-C) were measured.

### 2.4 Histopathological analysis

BAT samples from the interscapular region were excised and fixed in 4% paraformaldehyde. After dehydration, clearing, paraffin embedding, and sectioning, tissue slices were stained

with hematoxylin and eosin (H&E). The stained sections were examined and photographed under a light microscope (Leica, Vizla, Germany).

## 2.5 Quantitative PCR analysis

Total RNA was extracted from BAT using TRIzol reagent and reverse-transcribed into cDNA. Quantitative PCR was performed using the QuantStudio 5 Real-Time PCR System (Thermo Fisher Scientific, MA, USA). The thermal cycling conditions were: 50 °C for 2 min, 95 °C for 2 min, followed by 40 cycles of 95 °C for 15 s, 60 °C for 15 s, and 72 °C for 1 min. The housekeeping gene 36B4 was used as an internal control. Primer sequences are provided in Table 1.

## 2.6 Western blotting

BAT was lysed using RIPA lysis buffer. After protein concentration was determined using the BCA assay, 8 µg of protein per sample was loaded for SDS-PAGE electrophoresis. The membrane was blocked with 5% skim milk in TBST for 1 h at room temperature and then incubated overnight at 4 °C with primary antibodies: UCP1 (ab234430, Abcam, Cambridge, UK), adenosine 5'-monophosphate-activated protein kinase (AMPK) (ab32112, Abcam, Cambridge, UK), phospho-AMPK (#4186, CST, Boston, USA), PGC-1α (AP0774, Bioworld, Minnesota, USA), and tubulin (66031-1-Ig, Proteintech, Chicago, USA). After washing with TBST, membranes were incubated with the appropriate secondary antibodies at room temperature for 1 h, followed by additional

washes with TBST. Signals were visualized using ECL chemiluminescent substrate, and band intensities were quantified using ImageJ software.

## 2.7 RNA-sequencing

BAT samples from four randomly selected mice per group were used for RNA sequencing. Sequencing was performed by Annoroad Co., Ltd. using a high-throughput sequencing platform. Differentially expressed genes (DEGs) were identified based on the criteria:  $|\log_2 \text{fold change}| \geq 1.5$  and  $q\text{-value} \leq 0.05$ .

## 2.8 Function enrichment analysis

Identified DEGs were uploaded to the DAVID database (<https://david.ncifcrf.gov/>), with the species set to *Mus musculus*. Gene ontology (GO) functional enrichment and Kyoto encyclopedia of genes and genomes (KEGG) pathway enrichment analyses were performed with a significance threshold of  $P < 0.05$ . Enrichment bubble plots were generated using the online platform Bioinformatics (<https://www.bioinformatics.com.cn/>), and the results were visualized accordingly.

## 2.9 PPI network construction and hub genes screening

DEGs were submitted to the STRING database (<https://www.string-db.org/>) for protein-protein interaction (PPI) analysis. A confidence score  $\geq 0.7$  was applied, and disconnected nodes were excluded. The resulting network was imported into Cytoscape

Table 1 List of primers used for real-time quantitative PCR

Gene	Forward Primer (5'-3')	Reverse Primer (5'-3')
<i>Mfn1</i>	GATAAAGTCCTCCCCAGCGG	GCATGGGCCAGCTGATTAAC
<i>Mfn2</i>	TCCTCTCCCTCTGACACCTG	AAGGAGAGGGCGATGAGTCT
<i>Drp1</i>	GCCTCAGATCGTCGTAGTGG	TCAACTCCATTTTCTTCTCCTGT
<i>Fis1</i>	AGAGACGAAGCTGCAAGGAAT	CCGCTGTTCTCTTTGCTCC
<i>Ucp1</i>	TCAGGATTGGCCTCTACGAC	CTGTAGGCTGCCCAATGAAC
<i>Pgc1-α</i>	AGTGGTGTAGCGACCAATCG	GGGCAATCCGTCTTCATCCA
<i>Stip1</i>	ACCTGGGCACGAACTACAG	GGCATCATTTCCAGCTCCT
<i>Hsph1</i>	ATCTTCACCATCTCCACGGC	TTCTTGGCTTCTGGAGGCTG
<i>Mtor</i>	GGCCCAGGCAGAAAATTAC	GCGCTCTGCTCCTTGATTCT
<i>Prkag2</i>	GACCCTATCAGTGGGAACGC	CCTGACTCATCCACCACAGG
<i>Prkab1</i>	TTCGTGGATGGACAGTGGAC	CGGGGCTTTGAACCTCTCTT
<i>Foxo1</i>	GATAAGGGCGACAGCAACAG	CTCTTGCCTCCCTCTGGATTG
<i>Bag3</i>	CCCAACTGCTCATGGACCTG	GAGCTGGGTAGTGGGTCTTC
<i>Dnajb1</i>	ACGACGAGATCAAGCGAGC	GGGGTCTCCGTGGAATGTG
<i>Hspa1b</i>	CATGGTGCTGACGAAGATGA	GAGAGTCGTTGAAGTAGGCG
<i>36B4</i>	CGACCTGGAAGTCCAACCTAC	ATCTGCTGCATCTGCTTG

software, and the CytoNCA plug-in was used to calculate node degree and identify the top 10 hub genes.

## 2.10 Connectivity map

Upregulated and downregulated DEGs from the top 10 KEGG pathways were entered into the CMap database (<https://clue.io/>) for small-molecule drug prediction. The top 10 traditional Chinese medicine compounds were selected based on enrichment scores.

## 2.11 Cordycepin intervention

Male C57BL/6J mice were randomly divided into four groups ( $N = 10$  per group): a normal light-dark cycle group (LD), a continuous light group (LL), a low-dose cordycepin group (Cpn-L), and a high-dose cordycepin group (Cpn-H). Mice in the LD group were exposed to a 12 h:12 h light-dark cycle, while the LL, Cpn-L, and Cpn-H groups were exposed to continuous light (24 h: 0 h light-dark cycle). Cordycepin (purity  $\geq 98\%$ ; Shanghai Yuanye Bio-Technology Co., Ltd., Shanghai, China) was administered orally at 25 mg/kg in the Cpn-L group and 50 mg/kg in the Cpn-H group once daily for 5 weeks. The LD and LL groups received an equal volume of distilled water.

## 2.12 Statistical analysis

Statistical analyses were performed using GraphPad Prism 9.0.

Data are presented as mean  $\pm$  SEM. Normality and homogeneity of variance were tested prior to further analysis. One-way ANOVA was used for comparisons among multiple groups when assumptions were met; otherwise, the Kruskal-Wallis H test was applied. A  $P$ -value  $< 0.05$  was considered statistically significant.

## 3 Results

### 3.1 Continuous light exposure leads to dysregulation of lipid metabolism in mice

Following 5 weeks of continuous light exposure, no significant difference in body weight was observed between the LL group and the LD group (Fig. 1A). However, mice in the LL group exhibited significantly lower food intake compared to those in the LD group (Fig. 1B). Notably, despite the absence of body weight differences and a reduction in caloric intake, the body fat percentage in the LL group was significantly higher than that in the LD group (Fig. 1C), indicating a disruption in metabolic homeostasis induced by continuous light exposure. To further assess the effects of continuous light on systemic lipid metabolism, serum lipid profiles were examined. TG levels were significantly elevated in the LL group (Fig. 1D), whereas TC and HDL-C levels were significantly decreased (Fig. 1E and 1F). Although LDL-C levels were slightly reduced in the LL group, the difference did not reach statistical significance (Fig. 1G).

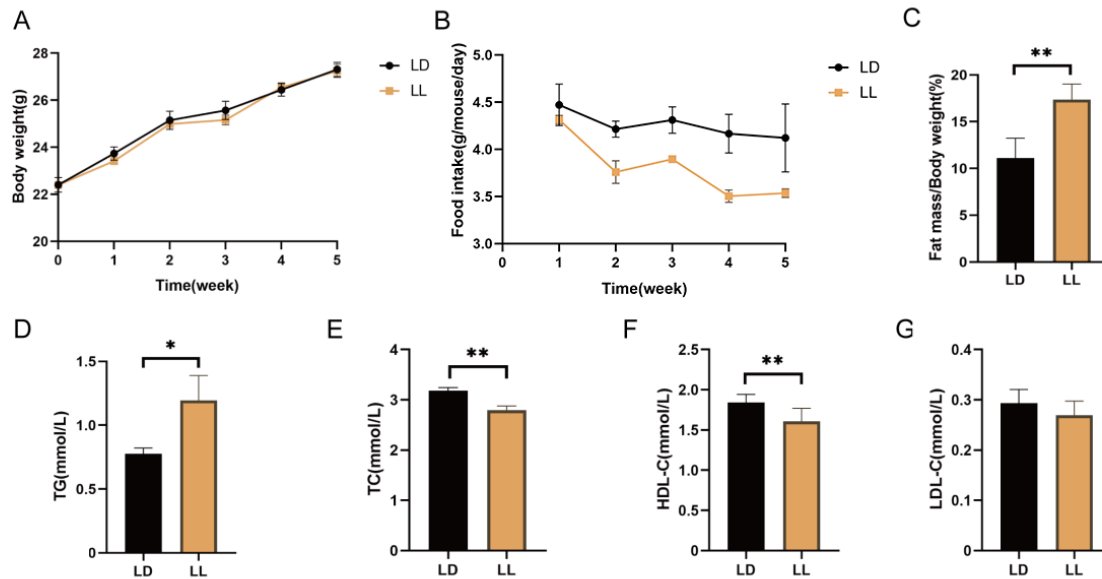


**Fig. 1** Continuous light exposure induces lipid metabolism disorders in mice

(A) Body weight; (B) Food intake; (C) Body fat percentage; (D) Serum levels of triglyceride (TG); (E) Total cholesterol (TC); (F) High density lipoprotein cholesterol (HDL-C); (G) Low density lipoprotein cholesterol (LDL-C). Data are presented as mean  $\pm$  SEM;  $N = 10$ /group. \* $P < 0.05$ , \*\* $P < 0.01$  vs. LD. LD, control group; LL, experimental group.

These findings suggest that prolonged exposure to continuous light impairs lipid metabolism, characterized by increased fat accumulation and altered serum lipid profiles, likely due to decreased energy expenditure.

### 3.2 Continuous light exposure leads to BAT whitening in mice

H&E staining revealed that, after 5 weeks of continuous light exposure, BAT morphology in mice changed from typical multi-locular small lipid droplets to large unilocular lipid droplets. Additionally, adipocyte size was significantly increased in the LL group compared to the LD group (Fig. 2A). To further assess mitochondrial function and thermogenic capacity, the mRNA expression levels of mitochondrial-related genes (*Mfn1*, *Mfn2*, *Drp1*, *Fis1*) and thermogenic markers (*Ucp1* and *Pgc-1 $\alpha$* ) in BAT were analyzed by RT-qPCR. The results showed that, apart from *Fis1*, the expression of these genes was significantly reduced in the LL group (Fig. 2B), suggesting impaired mitochondrial dynamics and thermogenesis. Western blot analysis further

confirmed that the protein expression level of UCP1, a key thermogenic marker specific to BAT, was markedly decreased in mice exposed to continuous light (Fig. 2C and 2D).

These findings indicate that continuous light exposure promotes the whitening of BAT, characterized by increased lipid droplet size, downregulation of mitochondrial and thermogenic gene expression, and reduced BAT activity.

### 3.3 Continuous light exposure alters the gene expression profile of BAT in mice

To investigate the molecular changes in BAT induced by continuous light exposure, RNA-seq was performed on BAT samples from LD and LL mice. A total of 363 DEGs were identified, including 151 upregulated and 212 downregulated genes in the LL group compared to the LD group (Fig. 3A-3C).

GO enrichment analysis revealed that the DEGs were primarily associated with biological processes such as regulation of

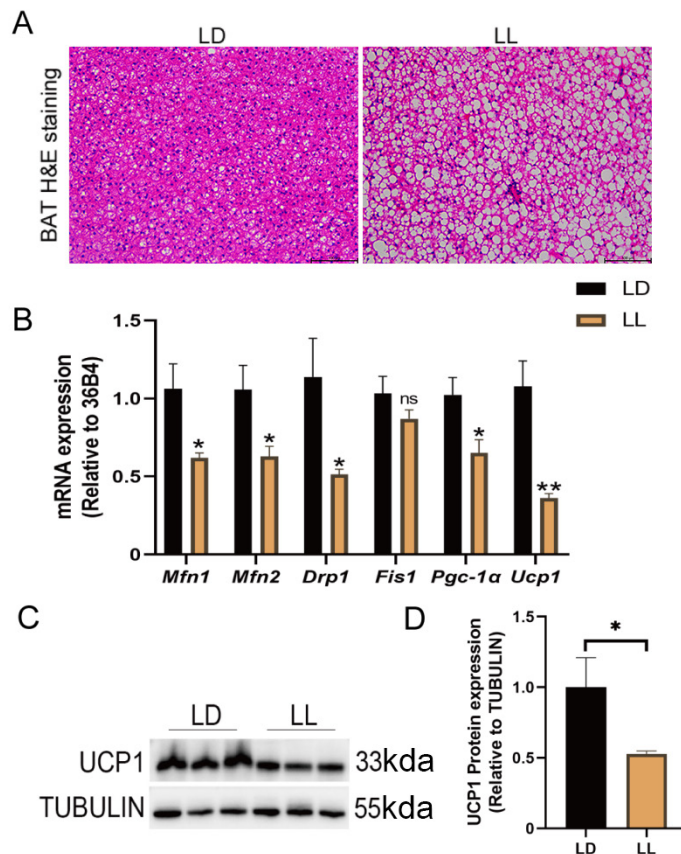


**Fig. 2** Continuous light exposure induces brown adipose tissue (BAT) whitening in mice

(A) Hematoxylin and Eosin (H&E) staining; (B) *Mfn1*, *Mfn2*, *Drp1*, *Fis1*, *Pgc-1 $\alpha$* , *Ucp1* mRNA levels; (C-D) western blot for uncoupling protein 1.  $N = 5-6/\text{group}$ ; \* $P < 0.05$ , \*\* $P < 0.01$  vs. LD. BAT, brown adipose tissue; UCP1, uncoupling protein 1.

protein kinase activity, lipid metabolism, fatty acid metabolism, and negative regulation of protein phosphorylation. In terms of cellular components, the DEGs were enriched in the interstitial matrix, external encapsulating structure, extracellular matrix, and cardiac myofibrils. Regarding molecular function, the DEGs were significantly enriched in activities such as MAP kinase tyrosine/serine/threonine phosphatase activity, enzyme binding, MAP kinase phosphatase activity, protein kinase C inhibitor activity, and heat shock protein binding (Fig. 3D). KEGG pathway enrichment analysis further showed that the DEGs were predominantly involved in pathways including biosynthesis of unsaturated fatty acids, insulin resistance, mitogen-activated protein kinases (MAPK) signaling, circadian rhythm, fatty acid elongation, AMPK signaling, alcoholic liver disease, apelin signaling, adipocytokine signaling, and peroxisome proliferator-activated receptor (PPAR) signaling (Fig. 3E).

These results demonstrate that continuous light exposure induces extensive transcriptional reprogramming in mouse BAT, affecting a wide range of biological processes and signaling pathways related to metabolism and cellular stress responses

### 3.4 PPI network construction and hub genes screening

To further identify core regulatory genes involved in BAT whitening under continuous light exposure, a PPI network of DEGs was constructed using the STRING database (Fig. 4A). After filtering for high-confidence interactions (confidence score  $\geq 0.7$ ) and removing unconnected nodes, the top 10 hub genes were identified using the Degree algorithm in Cytoscape: *Hspa1b*, *Dnajb1*, *Stip1*, *Hsph1*, *Mtor*, *Ppargc1a*, *Prkag2*, *Prkab1*, *Foxo1*, and *Bag3* (Fig. 4B).

These hub genes can be broadly categorized into two functional

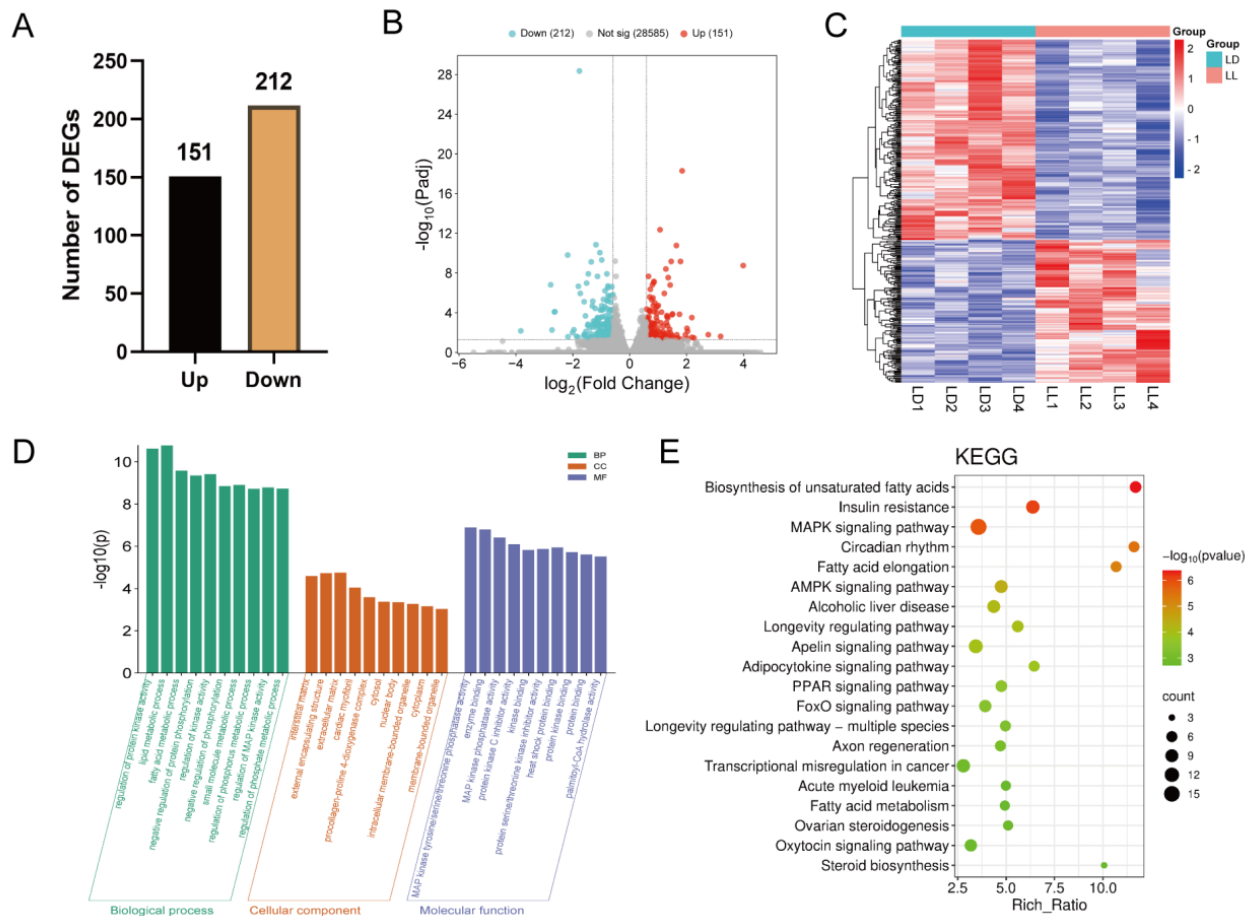


**Fig. 3** Functional enrichment analysis of differentially expressed genes (DEGs)

(A) Number of DEGs; (B) Volcanic maps; (C) Heat maps; (D) Gene ontology (GO) analysis; (E) Kyoto encyclopedia of genes and genomes (KEGG) analysis. LD, control group; LL, experimental group.

groups: those involved in the AMPK signaling pathway (*Mtor*, *Ppargc1a*, *Prkag2*, *Prkab1*, *Foxo1*) and those associated with the heat shock protein family (*Hspa1b*, *Dnajb1*, *Stip1*, *Hsph1*, *Bag3*). KEGG pathway enrichment analysis revealed that these hub genes were mainly associated with insulin resistance, AMPK signaling, adipocytokine signaling, glucagon signaling, apelin signaling, alcoholic liver disease, thermogenesis, and circadian rhythm pathways (Fig. 4C). These pathways overlap substantially with those enriched among the total set of 363 DEGs, suggesting that the identified hub genes may play pivotal roles in BAT whitening induced by continuous light.

Heatmap analysis showed that, with the exception of *Mtor* and *Prkab1*, the expression levels of the remaining hub genes were significantly upregulated in the LL group (Fig. 4D). RT-qPCR validation confirmed the RNA-seq results for six of the ten hub genes. Specifically, the expression of *Stip1*, *Bag3*, *Ppargc1a*, and *Foxo1* showed discrepancies between sequencing and qPCR data (Fig. 4E). Notably, the AMPK-related hub genes, *Mtor*, *Ppargc1a*, *Prkab1*, and *Foxo1*, were significantly downregulated in the LL group.

These findings suggest that the whitening of BAT caused by continuous light exposure is likely associated with suppression of the AMPK signaling pathway.

### 3.5 Cordycepin activates BAT through the AMPK / PGC-1 $\alpha$ / UCP1 pathway

To identify targeted therapeutic agents capable of alleviating BAT whitening induced by continuous light exposure, DEGs involved in the top 10 KEGG-enriched pathways were input into the CMap database (Supplementary Table 1). The top 10 traditional Chinese medicine compounds were identified (Table 2). Among them, cordycepin has been previously reported as an activator of the AMPK pathway, which plays a crucial role in regulating energy metabolism. Based on this and the earlier findings suggesting suppression of AMPK signaling during BAT whitening, it was hypothesized that cordycepin might reverse the whitening phenotype by reactivating the AMPK pathway.

After 5 weeks of cordycepin treatment, body weight, food intake, body composition, and serum lipid levels were evaluated in all groups. There was no significant difference in body weight among the groups (Fig. 5A). Food intake was not significantly different between the LL, Cpn-L, and Cpn-H groups, though all showed

Table 2 Traditional Chinese Medicine Compounds

Name	Score
resveratrol	0.5505
rotenone	0.5361
colchicine	0.5276
ellipticine	0.5112
cordycepin	0.4984
enoxolone	0.4771
pterostilbene	0.4736
scoulerine	0.4622
paclitaxel	0.4507
evodiamine	0.4507

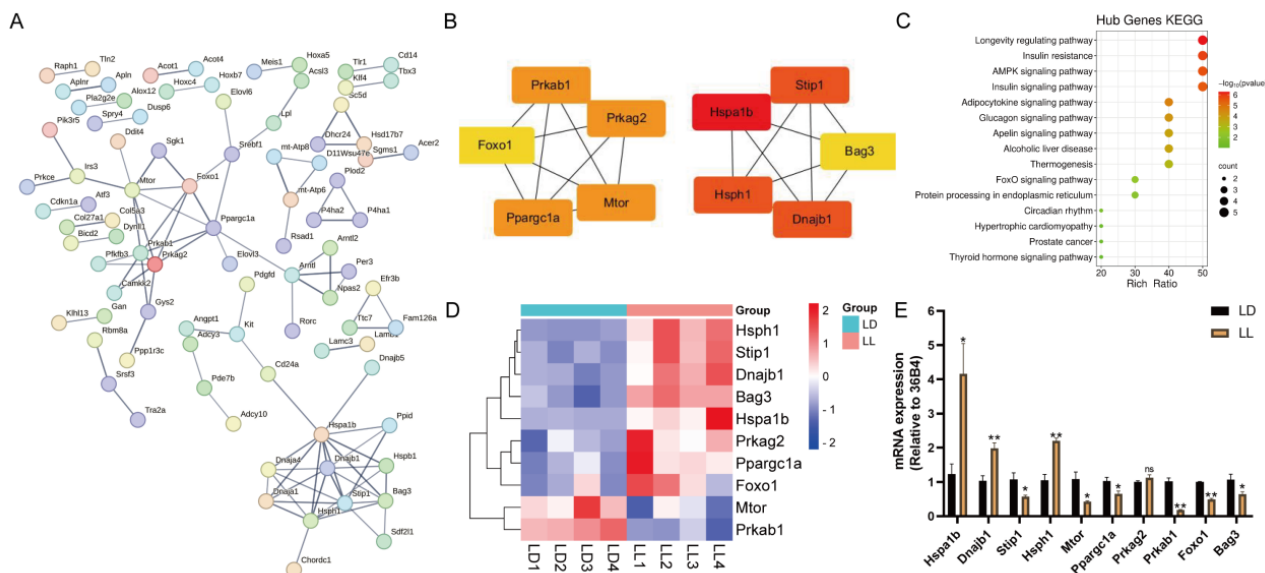
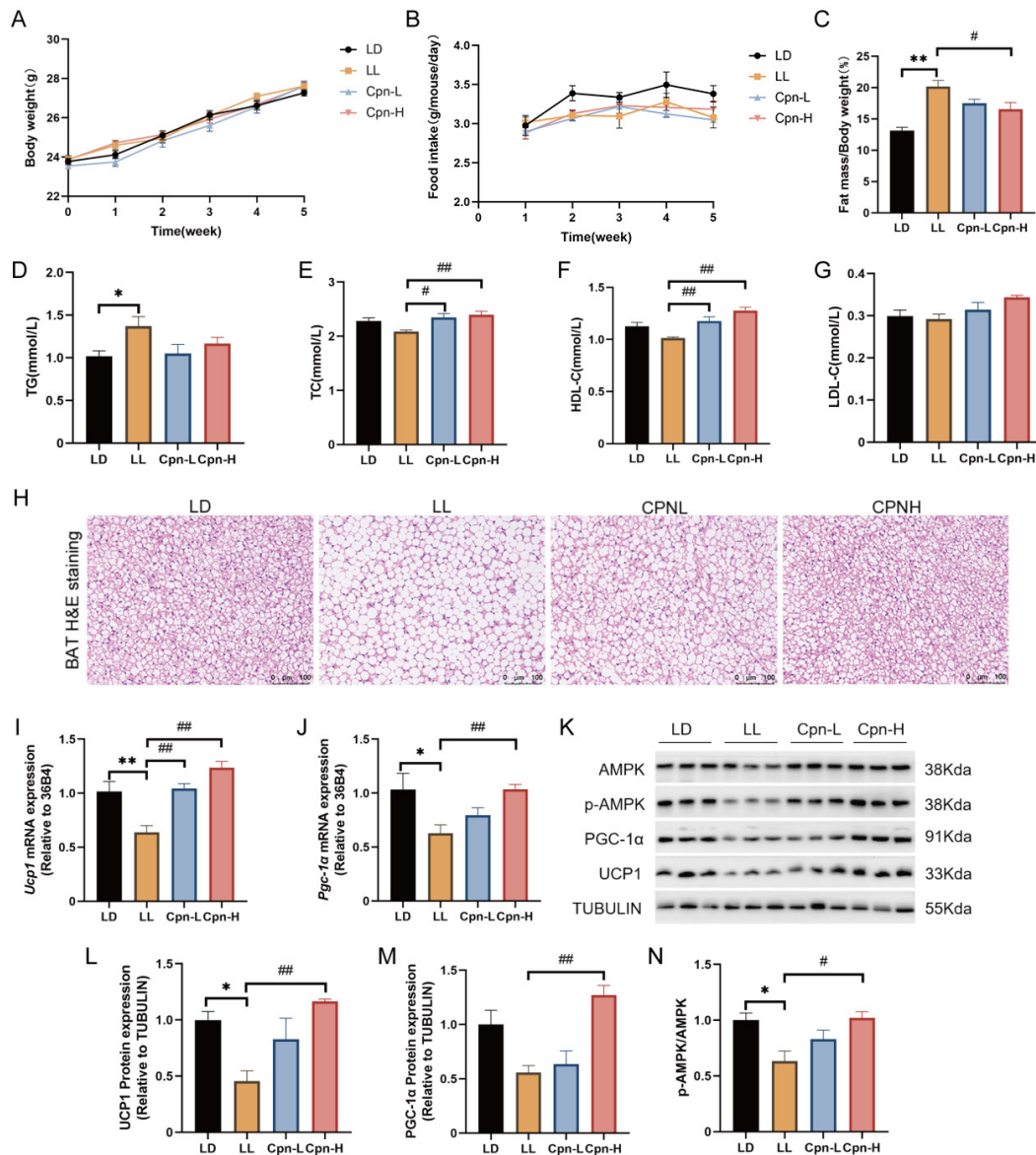


Fig. 4 Protein-protein interaction (PPI) network construction and hub genes screening (A) PPI network of differentially expressed genes (DEGs); (B) Hub genes of DEGs; (C) Kyoto encyclopedia of genes and genomes (KEGG) analysis of hub genes; (D) Heat maps of hub genes; (E) mRNA levels of hub genes. *N* = 5-6/group; \**P* < 0.05, \*\**P* < 0.01 vs. LD. LD, control group.

a trend toward reduction compared to the LD group (Fig. 5B). Mice in the LL group exhibited a significant increase in body fat percentage compared to the LD group, whereas the Cpn-H group showed a marked reduction in fat mass compared to the LL group (Fig. 5C), indicating that high-dose cordycepin effectively mitigates fat accumulation induced by continuous light. Serum lipid analysis revealed a trend toward improvement in lipid profiles

following cordycepin treatment, although the differences were not statistically significant (Fig. 5D-5G). Histological examination using H&E staining showed that BAT morphology in the treatment groups reverted to a multilocular pattern. Brown adipocytes in the Cpn-H group were smaller in size, further supporting the alleviation of BAT whitening (Fig. 5H).



**Fig. 5** Cordycepin activates brown adipose tissue through the adenosine 5'-monophosphate-activated protein kinase (AMPK)/PGC-1 $\alpha$ /uncoupling protein 1 (UCP1) pathway

(A) Body weight; (B) Food intake; (C) Fat mass; (D) Serum levels of triglyceride (TG); (E) Total cholesterol (TC); (F) High density lipoprotein (HDL-C); (G) Low density lipoprotein (LDL-C); (H) H&E staining; (I) *Ucp1* mRNA levels; (J) *Pgc-1 $\alpha$*  mRNA levels; (K-N) Western blot for AMPK, p-AMPK, UCP1 and PGC-1 $\alpha$ .  $N = 5-6/\text{group}$ ; \* $P < 0.05$ , \*\* $P < 0.01$  vs. LD; # $P < 0.05$ , ## $P < 0.01$  vs. LL. LD, control group; LL, experimental group.

To confirm whether cordycepin exerted its effects *via* the AMPK signaling pathway, the activation status of AMPK in BAT was assessed. Western blot analysis revealed a significant increase in phosphorylated AMPK levels following cordycepin administration. Furthermore, the expression of thermogenic markers UCP1 and PGC-1 $\alpha$  was upregulated in treated groups (Fig. 5I-5N).

These results indicate that cordycepin activates the AMPK/PGC-1 $\alpha$ /UCP1 signaling pathway, which may contribute to restoring BAT thermogenic function, inhibiting its whitening, and thereby improving systemic metabolic balance under continuous light exposure (Fig. 6).

## 4 Discussion

Light is a fundamental environmental cue essential for maintaining biological rhythms and physiological processes. The Earth's rotation creates a natural 24 h light-dark cycle, which organisms have adapted to over evolutionary time. However, in polar regions, extreme photoperiodic conditions such as polar day and polar night significantly disrupt this rhythm. These atypical light environments can profoundly affect both physiological and psychological health in individuals working in these regions. In this study, we aimed to simulate polar day conditions by subjecting mice to continuous artificial lighting for 5 weeks and evaluating the resulting metabolic changes.

Our findings revealed that continuous light exposure reduced food intake, increased body fat percentage, elevated serum levels of TG, and decreased HDL-C in mice. These changes indicate a disruption in systemic metabolic balance. BAT, known for its role in non-shivering thermogenesis and energy expenditure, has become

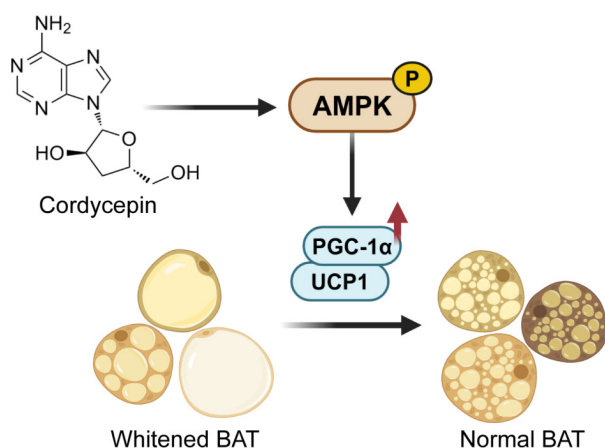


**Fig. 6** Schematic diagram illustrating the proposed mechanism of brown adipose tissue (BAT) activation by cordycepin

AMPK, adenosine 5'-monophosphate-activated protein kinase; UCP1, uncoupling protein 1.

a promising target for the treatment of metabolic disorders<sup>[17-18]</sup>. However, our results demonstrate that continuous light impairs BAT activity and structure. After 5 weeks of exposure, BAT underwent morphological changes from multilocular to unilocular lipid droplets, accompanied by a significant enlargement of adipocytes. Concurrently, expression levels of mitochondrial fusion and fission genes (*Mfn1*, *Mfn2*, *Drp1*) and thermogenic genes (*Pgc-1 $\alpha$* , *Ucp1*) were markedly downregulated, indicating impaired mitochondrial function and reduced thermogenic capacity. Such whitening of BAT may result in diminished energy expenditure and contribute to systemic metabolic imbalance, suggesting that BAT whitening is a key pathological feature in light-induced metabolic disruption. Identifying the molecular mechanisms and therapeutic targets of BAT whitening may provide new strategies for restoring metabolic homeostasis.

To elucidate the molecular underpinnings of BAT whitening, we performed RNA-seq analysis and identified 363 DEGs in response to continuous light exposure. KEGG enrichment analysis revealed that these DEGs were mainly associated with pathways regulating energy metabolism, including the biosynthesis of unsaturated fatty acids, insulin resistance, MAPK signaling, circadian rhythm, fatty acid elongation, AMPK signaling, and adipocytokine signaling. These results further underscore the impact of light-induced stress on energy balance and BAT function.

Through PPI analysis, we identified 10 hub genes: *Hspa1b*, *Dnajb1*, *Stip1*, *Hsph1*, *Bag3*, *Mtor*, *Ppargc1a*, *Prkag2*, *Prkab1*, and *Foxo1*. Literature review indicated that *Hspa1b*, *Dnajb1*, *Stip1*, *Hsph1*, and *Bag3* belong to the heat shock protein family. RT-qPCR validation confirmed elevated expression of *Hspa1b*, *Dnajb1*, and *Hsph1*, suggesting a stress response. Heat shock proteins function as molecular chaperones involved in protein folding, transport, degradation, and protection against stress-induced damage. They also regulate apoptosis, immune responses, and signal transduction<sup>[19-21]</sup>. Thus, their upregulation in BAT may represent a compensatory response to light-induced cellular stress.

The remaining hub genes, *Mtor*, *Ppargc1a*, *Prkag2*, *Prkab1*, and *Foxo1*—are closely associated with the AMPK signaling pathway, a central regulator of cellular energy homeostasis. AMPK is a heterotrimeric serine/threonine kinase that senses cellular energy status and maintains metabolic balance. In our study, the expression of *Prkab1*, *Mtor*, *Foxo1*, and *Ppargc1a* was downregulated following continuous light exposure.

*Prkab1*, encoding the  $\beta$  subunit of AMPK, has been shown to suppress inflammation, fatty acid and cholesterol synthesis, and atherosclerosis when activated<sup>[22]</sup>. *Mtor*, a key negative regulator of autophagy, is directly inhibited by AMPK *via* phosphorylation of

the Raptor subunit, promoting autophagy and energy preservation under stress<sup>[23-24]</sup>. *Foxo1* is a downstream target of AMPK and regulates gluconeogenesis; its activity is inhibited when phosphorylated by AMPK, thereby reducing expression of genes such as *G6Pase* and *Pepck*<sup>[25]</sup>. *Pgc-1 $\alpha$*  plays a critical role in mitochondrial biogenesis and thermogenesis in BAT and is activated *via* phosphorylation by AMPK, ultimately promoting *Ucp1* expression and heat generation<sup>[26-28]</sup>. Collectively, these findings support that AMPK pathway inhibition is a key mechanism driving BAT whitening under continuous light exposure and identify AMPK activation as a rational therapeutic strategy.

To explore potential interventions, we screened TCM compounds using the CMap database. Among the top 10 candidates, rotenone, colchicine, ellipticine, scoulerine, paclitaxel, and evodiamine were excluded due to known toxicities. Resveratrol, pterostilbene, and cordycepin, all known AMPK activators<sup>[29-31]</sup>, were further evaluated. While resveratrol and pterostilbene have been widely studied and shown to activate BAT and promote WAT browning<sup>[32-34]</sup>, the effects of cordycepin on BAT were previously unknown. Cordycepin possesses higher bioavailability, broader pharmacological effects, and lower toxicity compared to the others, making it a promising candidate for further investigation.

Cordycepin, a nucleoside analog derived from fungi such as *Cordyceps militaris*, has been shown to inhibit lipid droplet synthesis by downregulating genes such as *Fsp27* and *Perilipin1*, and to activate AMPK in WAT, thereby promoting browning through upregulation of *Pgc-1 $\alpha$* , *Ucp1*, *Cidea*, and *Cpt1b*<sup>[35-36]</sup>. Based on these properties, we hypothesized that cordycepin might activate BAT *via* the AMPK/PGC-1 $\alpha$ /UCP1 pathway. Our experimental results confirmed this hypothesis: cordycepin restored the multilocular morphology of BAT, increased phosphorylated AMPK levels, and significantly upregulated the expression of *Pgc-1 $\alpha$*  and *Ucp1* at both the gene and protein levels.

Finally, it is important to note the potential role of the nervous system in mediating light-induced BAT dysfunction. Light has been shown to activate intrinsically photosensitive retinal ganglion cells, which transmit signals *via* the optic nerve to hypothalamic and medullary nuclei. These, in turn, regulate BAT through the sympathetic nervous system (SNS), ultimately reducing thermogenesis<sup>[37-38]</sup>. Thus, disruption of the retina-hypothalamus-SNS axis may represent an upstream mechanism for AMPK suppression and BAT whitening. Future research should explore this neuroendocrine axis as a therapeutic target, investigating whether modulation of neural circuits can reverse metabolic dysfunction caused by abnormal light exposure.

In summary, our study demonstrates that prolonged continuous light exposure impairs BAT function through inhibition of the AMPK/PGC-1 $\alpha$ /UCP1 signaling pathway, leading to increased fat accumulation and lipid metabolism disorders. Cordycepin effectively activates AMPK signaling, restores BAT thermogenic function, and represents a promising candidate for mitigating light-induced metabolic disturbances. These findings provide new insights into the pathophysiology of light-driven metabolic dysregulation and lay the groundwork for developing effective preventive and therapeutic strategies.

## 5 Conclusion

In conclusion, this study demonstrates that continuous light exposure induces whitening of BAT and disrupts systemic metabolic homeostasis, primarily through inhibition of the AMPK signaling pathway in BAT. Furthermore, we show that cordycepin significantly alleviates the increase in body fat percentage and the decline in BAT activity caused by continuous light, likely *via* activation of the AMPK/PGC-1 $\alpha$ /UCP1 signaling cascade. These findings not only elucidate the molecular mechanisms underlying light-induced BAT dysfunction but also identify cordycepin as a promising therapeutic agent. This work offers a novel mechanistic framework and potential intervention strategy for managing metabolic dysregulation associated with prolonged light exposure.

## Acknowledgments

Not applicable.

## Research ethics

All animal procedures were conducted in accordance with institutional guidelines for the care and use of laboratory animals at the Institute of Military Medical Sciences Academy. The experimental protocol was approved by the Experimental Animal Ethics Committee of the Academy of Military Medical Sciences (IACUC of AMMS-04-2023-034, 10 October 2023).

## Informed consent

Not applicable.

## Author contributions

Zhang R N: Conceptualization, data curation, visualization, writing original draft. Zhang L: Conceptualization, writing, original draft. Jiang Y Q: Visualization, formal analysis. Zhao Z W: Software. Zhang G Y: Formal analysis. Zhang Y Q: Formal analysis. Wu S: Data curation. Li X: Project administration, writing, review and editing. Yang D F:

Project administration, writing, review and editing.

## Use of large language models, AI and machine learning tools

Not applicable.

## Conflict of interest

Yang D F is an Editorial Board Member of Frigid Zone Medicine. The article was subject to the journal's standard procedures, with peer review

handled independently of this Member and his research groups.

## Research funding

Not applicable.

## Data availability

The original contributions presented in this study are included in the article. Further inquiries can be directed to the corresponding authors.

## References

- [1] Kolomeichuk S N, Korostovtseva L S, Morozov A V, *et al.* Comparative analysis of sleep hygiene and patterns among adolescents in two Russian Arctic regions: a pilot study. *Children (Basel)*, 2024; 11(3): 279.
- [2] Thuany M, Viljoen C, Gomes T N, *et al.* Antarctic expeditions: a systematic review of the physiological, nutritional, body composition and psychological responses to treks across the continental ice. *Sports Med*, 2024; 55(5): 1145-1163.
- [3] Maciejczyk M, Arazny A, Opyrchal M. Changes in aerobic performance, body composition, and physical activity in polar explorers during a year-long stay at the polar station in the Arctic. *Int J Biometeorol*, 2017; 61(4): 669-675.
- [4] Xu Y J, Xie Z Y, Gong Y C, *et al.* The association between outdoor light at night exposure and adult obesity in Northeastern China. *Int J Environ Health Res*, 2024; 34(2): 708-718.
- [5] Sakers A, De Siqueira M K, Seale P, *et al.* Adipose-tissue plasticity in health and disease. *Cell*, 2022; 185(3): 419-446.
- [6] Cedikova M, Kripnerová M, Dvorakova J, *et al.* Mitochondria in white, brown, and beige adipocytes. *Stem Cells Int*, 2016; 2016: 6067349.
- [7] Lee P, Bova R, Schofield L, *et al.* Brown adipose tissue exhibits a glucose-responsive thermogenic biorhythm in humans. *Cell Metabolism*, 2016; 23(4): 602-609.
- [8] Kuipers E N, Held N M, In Het Panhuis W, *et al.* A single day of high-fat diet feeding induces lipid accumulation and insulin resistance in brown adipose tissue in mice. *Am J Physiol Endocrinol Metab*, 2019; 317(5): E820-E830.
- [9] Pan X X, Yao K L, Yang Y F, *et al.* Senescent T cell induces brown adipose tissue "whitening" via secreting IFN-gamma. *Front Cell Dev Biol*, 2021; 9: 637424.
- [10] Hao L, Khan M S H, Zu Y, *et al.* Thermoneutrality inhibits thermogenic markers and exacerbates nonalcoholic fatty liver disease in mice. *Int J Mol Sci*, 2024; 25(15): 8482.
- [11] Bolin A P, De Fatima Silva F, Salgueiro R B, *et al.* Glucocorticoid modulates oxidative and thermogenic function of rat brown adipose tissue and human brown adipocytes. *J Cell Physiol*, 2024; 239(9): 1-12.
- [12] Kooijman S, Van Den Berg R, Ramkisoensing A, *et al.* Prolonged daily light exposure increases body fat mass through attenuation of brown adipose tissue activity. *Proc Natl Acad Sci U S A*, 2015; 112(21): 6748-6753.
- [13] Li X, Xiong X, Yi C. Epitranscriptome sequencing technologies: decoding RNA modifications. *Nat Methods*, 2016; 14(1): 23-31.
- [14] Du K, Chen G H, Bai X, *et al.* Dynamics of transcriptome and chromatin accessibility revealed sequential regulation of potential transcription factors during the brown adipose tissue whitening in rabbits. *Front Cell Dev Biol*, 2022; 10: 981661.
- [15] Lyu J, Liu Y, Liu F, *et al.* Therapeutic effect and mechanisms of traditional Chinese medicine compound (Qilong capsule) in the treatment of ischemic stroke. *Phytomedicine*, 2024; 132: 155781.
- [16] Huang W, Yu P, Zhao X, *et al.* CMAP prediction and experimental validation of Forskolin as a podocyte protective and anti-proteinuric drug for nephrotoxic serum-treated mice. *Biochem Pharmacol*, 2025; 232: 116727.
- [17] Markina N O, Matveev G A, Zasyupkin G G, *et al.* Role of brown adipose tissue in metabolic health and efficacy of drug treatment for obesity. *J Clin Med*, 2024; 13(14): 4151.
- [18] Carpentier A C, Blondin D P, Virtanen K A, *et al.* Brown Adipose Tissue Energy Metabolism in Humans. *Front Endocrinol (Lausanne)*, 2018; 9: 447.
- [19] Li Y, Cao S, Li Y. Mechanistic study of heat shock protein 60-mediated apoptosis in DF-1 cells. *Poult Sci*, 2024; 103(6): 103619.
- [20] Zininga T, Ramatsui L, Shonhai A. Heat shock proteins as immunomodulators. *Molecules*, 2018; 23(11): 2846.
- [21] Wong S H D, Yin B, Li Z, *et al.* Mechanical manipulation of cancer cell tumorigenicity via heat shock protein signaling. *Sci Adv*, 2023; 9(27): 9593.
- [22] Day E A, Townsend L K, Rehal S, *et al.* Macrophage AMPK  $\beta$ 1 activation by PF-06409577 reduces the inflammatory response, cholesterol synthesis, and atherosclerosis in mice. *iScience*, 2023; 26(11): 108269.
- [23] Cheng Y, Mei X, Shao W, *et al.* Nobiletin alleviates macrophage M2 polarization by activating AMPK-mTOR-mediated autophagy in pulmonary fibrosis mice. *Int Immunopharmacol*, 2024; 139: 112792.
- [24] Shen B, Wen Y, Li S, *et al.* Paeonol ameliorates hyperlipidemia and autophagy in mice by regulating Nrf2 and AMPK/mTOR pathways. *Phytomedicine*, 2024; 132: 155839.
- [25] Wu F, Lu F, Dong H, *et al.* Oxyberberine inhibits hepatic gluconeogenesis via AMPK-mediated suppression of FoxO1 and CRTCL2 signaling axes. *Phytother Res*, 2024, Online ahead of print.
- [26] Sagliocchi S, Schiano E, Acampora L, *et al.* AbaComplex enhances

mitochondrial biogenesis and adipose tissue browning: implications for obesity and glucose regulation. *Foods*, 2024; 14(1): 48.

[27] Tang X, Shi Y, Chen Y, *et al.* Tetrahydroberberrubine exhibits preventive effect on obesity by activating PGC1 $\alpha$ -mediated thermogenesis in white and brown adipose tissue. *Biochemical pharmacology*, 2024; 226: 116381.

[28] Zhang Y Q, Zhang Z Z, Zhang Y W, *et al.* Baicalin promotes the activation of brown and white adipose tissue through AMPK/PGC1 $\alpha$  pathway. *Eur J Pharmacol*, 2022; 922: 174913.

[29] Wang H, An Y, Rajput S A, *et al.* Resveratrol and (-)-epigallocatechin-3-gallate regulate lipid metabolism by activating the AMPK pathway in hepatocytes. *Biology*, 2024; 13(6): 368.

[30] Lan T, Yu Y, Zhang J, *et al.* Cordycepin ameliorates nonalcoholic steatohepatitis by activation of the AMP-activated protein kinase signaling pathway. *Hepatology*, 2021; 74(2): 686-703.

[31] Shen B, Wang Y, Cheng J, *et al.* Pterostilbene alleviated NAFLD via AMPK/mTOR signaling pathways and autophagy by promoting Nrf2. *Phytomedicine: international journal of phytotherapy and phytopharmacology*, 2023; 109: 154561.

[32] Gómez-garcía I, Fernández-quintela A, Portillo M P, *et al.* Changes

in brown adipose tissue induced by resveratrol and its analogue pterostilbene in rats fed with a high-fat high-fructose diet. *J Physiol Biochem*, 2024; 80(3): 627-637.

[33] Yan H, Shao M, Lin X, *et al.* Resveratrol stimulates brown of white adipose via regulating ERK/DRP1-mediated mitochondrial fission and improves systemic glucose homeostasis. *Endocrine*, 2025; 87(1): 144-158.

[34] Nagao K, Jinnouchi T, Kai S, *et al.* Pterostilbene, a dimethylated analog of resveratrol, promotes energy metabolism in obese rats. *J Nutr Biochem*, 2017; 43: 151-155.

[35] Xu H, Wu B, Wang X, *et al.* Cordycepin regulates body weight by inhibiting lipid droplet formation, promoting lipolysis and recruiting beige adipocytes. *J Pharm Pharmacol*, 2019; 71(9): 1429-1439.

[36] Qi G, Zhou Y, Zhang X, *et al.* Cordycepin promotes browning of white adipose tissue through an AMP-activated protein kinase (AMPK)-dependent pathway. *Acta Pharm Sin B*, 2019; 9(1): 135-143.

[37] Meng J J, Shen J W, Li G, *et al.* Light modulates glucose metabolism by a retina-hypothalamus-brown adipose tissue axis. *Cell*, 2023; 186(2): 398-412.e17.

[38] Rao F, Xue T. Circadian-independent light regulation of mammalian metabolism. *Nat Metab*, 2024; 6(6): 1000-1007.